Incompressible airfoil shape optimization using NURBS parameterization

Ritin Mathews, Yajat Pandya and Matteo Puccioni

***Abstract*—The operative life of an aerodynamic structural element is characterized by standards demanding for high performances from the airfoil section of the wing in terms of aerodynamic loads; applications of this requirements are given by automobile rear wings, civil and military aircraft, Horizontal Axis Wind Turbines (HAWT) etc. In this work we define a shape optimization tool for airfoil sections typically used for incompressible flows. Starting from a user-defined objective function based on the aerodynamic loads acting on the airfoil, a commonly used Non-Uniform Rational B-Spline (NURBS) parametrization is used to shape the airfoil ([1], [2]). The design variables are given by the control points of the NURBS parametrization; this allows us both to keep a close control of the local shape and also to work with a low number of design variables (typically less than 10 for each side of the airfoil ([1])). The flow characteristics for an airfoil curve are evaluated using an analytical airfoil model for incompressible flows. Finally, a pre-defined MATLAB optimization tool is used to achieve the best airfoil shape. Different combinations for design parameters are considered by focusing either on the NURBS control points or the related weights ([3]). The results from previous studies are compared with a new constraint formulation where the streamwise and spanwise locations of the control points are fixed and only the normal coordinate and the weights are varied; this allows for a further reduction of the computational time.**

***Index Terms*—NURBS, airfoil, optimization.**

I. Introduction

IN In the last few decades large efforts have been made to develop optimization tools able to improve the aerodynamic performances of the aircraft acting on the shape of the airfoils (e.g. [4], [5], [6]). Among the several methods available in literature, the Non-Uniform Rational B-Spline (NURBS) approach has been widely used due to its low implementation cost and design freedom ([7]). The general idea underlying the aerodynamic optimization problem is to establish a target performance of the airfoil for a given design mission and modify iteratively the airfoil geometry in order to achieve such a target; at each iteration, the flow is solved through a suitable numerical technique, while the optimal direction is sought by means of a pre-defined optimization strategy. Here, some of the most important studies mentioning the basic features of this optimization framework will be reviewed.

The work of [3] focused on the comparison between the NURBS and the discretized approximations of the airfoil shape. In particular, the authors leveraged a pre-optimization problem where a set of given airfoils had to be reproduced by means of a certain parametrization technique; for the NURBS approximation, the authors found a mean deviation error of 10^{-5} between the target and the approximated airfoil using a maximum of 13 control points (and related weights) as design parameters. For the discretized method, the same accuracy was achieved with 150 points. Thus, the NURBS parametrization was shown to be the best to run optimization problems for real scenarios. For the latter, a target pressure distribution was assumed as objective function; the optimization strategy was based on a quasi-Newton searching technique, whereas the pressure around the airfoil was obtained through a flow solver for the transonic regime. Both 2D and 3D cases were considered; for all of them, a high level of accuracy was achieved when the pressure coefficient had to be replicated modifying the NURBS control points.

In the study of [1] the optimization of a transonic wing section was carried on based on the NURBS parametrization of the airfoil shape. In particular, the authors defined an optimization problem where the multi-objective robust cost function was defined as the trade off between the lift and drag forces obtained solving the flow around the airfoil; two different flight conditions were considered, namely steady climb and leveled cruise in the transonic regime. For each value of the weights associated to the multi-objective function, the NURBS control points were iteratively moved in order to achieve the global minimum. Subsequently, the Pareto frontier was defined for the present problem and, for a specific non-dominated solution, the authors found a substantial increase of the lift coefficient and drag reduction with respect to the initial airfoil shape.

[2] focused on the most sensitive design node coordinates for the design vector in the optimization model. They fixed the trailing edge nodes and created a sub-problem of estimating the optimum angle of attack, α, for each design vector. For a 2D problem, a total of 26 design points (13 NURBS control points with $x-y$ coordinates) were formulated, which reduced to 13 after conducting a sensitivity analysis. The Sequential Quadratic Programming (SQP) approach was chosen for the optimization process due to its robustness. Because of computational limitations, the objective of the problem was focused to optimizing an existing standard airfoil profile (local optimum) as opposed to finding the best possible profile (global optimum). This was also evident from the fact that most aerodynamic objectives are not necessarily smooth with respect to the design parameters.

The study of [8] focused on a genetic algorithm (GA) modified to work with real-valued variables in order to optimize the shape of a small wind turbine blade to maximize its efficiency. For incompressible flow conditions (chord Reynolds number equal to $200,000$), the blade section was parametrized with a Bezier curve (which can be seen as a particular case of

the NURBS parametrization) and the flow was solved with a very low computational effort using the XFOIL software. The reliability of this solver was tested a posteriori comparing several aerodynamic characteristics (namely pressure coefficient, lift coefficient, drag coefficient and efficiency) calculated either with XFOIL or the ANSYS CFX solver or evaluated experimentally through wind tunnel measurements. A large agreement was found for all the examined quantities, leading to the conclusion that an open-source low-cost solver is suitable for the present purpose provided adequate meshing and turbulence model. Furthermore, the optimized airfoil was shown to perform better than the commercial shapes in terms of lift coefficient and efficiency for a typical range of angles of attack ($4°$to $13°$); this also proved the insensitivity of the optimal operative point to different flow conditions, which is an essential feature for a robust optimal design technique.

Limited to theoretical models for 2D cases, various options are available such as like thin-airfoil theory and vortex lattice methods. These are typically used for incompressible, steady 2D flows where the angle of attack is small ([9]). The primary assumption for the applicability of thin-airfoil theory is the absence of significant flow separation at the trailing edge of an airfoil, which is useful to approximate a potential flow around the object. The airfoil curve is divided into a finite number of node points with a variable vortex strength at each point. Using basic fluid mechanics principles of no-slip and lift-circulation relationship, the induced velocity at each node point is estimated and equated to the integral of vorticity from the remaining nodes. This analytical formulation requires the geometry of the mean camber line of an airfoil, which can be directly estimated from a 2D shape (eg. NURBS) for the current work. In the context of airfoil design optimization, the flow around the airfoil can be estimated using this theory and the required constraints can be calculated. Such a method is then suitable to be integrated in the shape optimizer using steady incompressible and low angle of attack as main assumptions.

The rest of the report is drafted as follows: II describes the NURBS shape parametrization of an airfoil for reducing the design points. III describes the optimization objective function and corresponding aerodynamic constraints. The XFOIL MATLAB package and its implementation in the optimization process is also explained in this section. The choice of the initial airfoil, optimization results and the Pareto frontier are later explained in IV. Finally, V describes the conclusions and overall summary of the project.

December 1, 2020

II. The NURBS parametrization

A Non-Uniform Rational B-Spline (NURBS) curve $\mathbf{C}$ is defined starting from a sequence of $n+1$ control points $\mathbf{Q}_i = (X,\ Y,\ Z)$ and a parameter $u \in [0,\ 1]$ as follows ([7]):

$$\mathbf{C}(u) = \frac{\sum_{i=0}^{n} N_{i,p}(u) w_i \mathbf{Q}_i}{\sum_{i=0}^{n} N_{i,p}(u) w_i}. \tag{1}$$

Here, p is the order of the NURBS curve and $w_i \geq 0$ are the weights associated to each control points. The basis functions $N_{i,p}$ are based on a knot vector U whose dimension is $m+1$ defined as:

$$U = (\underbrace{0, ..., 0}_{p+1}, u_{p+1}, ..., u_{m-p-1}, \underbrace{1, ..., 1}_{p+1}). \tag{2}$$

The dimension of the knot vector is related to the number of control points and NURBS order by: $n = m - p - 1$ ([7]). The i-th basis of order p is a piece-wise polynomial function defined over the interval $(u_i,\ u_{i+p+1})$ and calculated recursively starting from $N_{i,0}(u)$:

$$N_{i,0}(u) = \begin{cases} 1 \text{ if } u_i \leq u \leq u_{i+1} \\ 0 \text{ otherwise} \end{cases} ; \tag{3}$$

then:

$$N_{i,p}(u) = \frac{u - u_i}{u_{i+p} - u_i} N_{i,p-1}(u) + \frac{u_{i+p+1} - u}{u_{i+p+1} - u_{i+1}} N_{i+1,p-1}(u). \tag{4}$$

Consequently, for each value of u, a point is individuated along the NURBS curve within the control segment $[\mathbf{Q}_0, ..., \mathbf{Q}_n]$. In particular, as $u = 0$ we have: $\mathbf{C}(0) = \mathbf{Q}_0$ whereas for $u = 1$, $\mathbf{C}(1) = \mathbf{Q}_n$. From (3) and (4), it can be inferred that any basis $N_{i,p}(u)$ evaluated on a node u_i is $p - k$ times differentiable, where k is the multiplicity of the node. Thus, to ensure the highest level of continuity of the basis function (and of the NURBS curve), in this study each internal node has multiplicity 1, whereas the external nodes ($u = 0,\ 1$) have multiplicity $p+1$. For the present problem, the NURBS curves have been evaluated through the MATLAB open-source toolbox of [10].

III. Optimization problem

A. Objective function formulation

For automotive applications,e specially for high performance race cars, the aerodynamics play an important role in on road or track performance. The side-view profile of a race car is similar to an airfoil i.e. a higher curvature on the top surface and lower one at the bottom. This generates lift as air flows over the surfaces. Since wheel traction to the road is primarily a function of net normal force (equal to the weight for a steady motion on a horizontal surface) it is critical to mitigate the lift generated by the airflow. It is even more advantageous if there was a device that could increase the net normal force, which is exactly the function of an automotive wing. In particular, by generating downforce using a wing, the vehicle performance (acceleration, braking and cornering) improves due the added traction.

Even though, in theory, it is advantageous to have as much downforce as possible, there are drawbacks. The air flowing over the front half of the vehicle still generates lift as earlier mentioned. Combined with this, the downforce generated by the wing will produce a pitching moment on the vehicle. Due to this phenomenon, the overall lift generated by the vehicle increases (similarly to an airfoil experiencing higher lift at higher angles of attack below stalling point). This is an extremely unfavorable situation as it is a positive feedback

loop. Such an event is avoided by additional inverted wing-like structures at the front end, (e.g. cannards, splitters etc). Due to such an issue, the downforce generated by the rear wing is usually favored to be in some optimal range. In this study, the range of lift coefficient (C_L) is usually set to be from 1.2 to 2.8 and the drag coefficient (C_D) is limited to 0.2 [11].

An automotive wing, while in operation, experiences various loads that generates material stress. The main aerodynamic loads are the downforce and the drag. Along with this, there exists a rotational moment about the span-wise axis that tends to increase the angle of attack. All these loads generate stresses namely - bending, shear and torsional stress. The analysis of the stress distributions created by the downforce and drag over an aerodynamic element is of primary importance to ensure the durability of the structure ([12], [13]). Clearly, a thick airfoil section would benefit of the large moment of inertia to decrease the level of bending, shear and torsional stress acting on the section. On the other hand, this would result in a weight increase which might be prohibitive for many applications ([14]). Thus, any structural wing optimization must necessarily take into account the weight reduction as primary requirement to justify the implementation of the optimized shape. A multi-objective problem is the most common way used to find a trade-off between the structural and the weight requirements in the context of aerodynamic element design ([15]). Thus, a two-objective function is formulated in problem based on structural and weights requirements:

$$\begin{array}{cc} \min_{\mathbf{Y}} & \left[\mu_1 A(\mathbf{Y}) + \mu_2 \frac{1}{J_{AC}(\mathbf{Y})}\right], \\ \text{subject to:} & 1.5 \leq C_L \leq 2.8 \\ & C_D \leq 0.2. \end{array} \tag{5}$$

In equation 5, $\mathbf{Y}$ is the vector of the vertical coordinates of the NURBS control points defining the airfoil, A is the area of the airfoil (directly proportional to the airfoil mass) and J_{AC} is the polar moment of inertia calculated with respect to the aerodynamic center (AC), which is directly related to the torsional stiffness of the section. For a multi-objective formulation, the weights $\mu_1,\ \mu_2$ are chosen between 0 and 1 such that: $\mu_1 + \mu_2 = 1$. The inequality constraints are focused on the aerodynamic features of the airfoil as previously explained.

To evaluate the multi-objective cost function, let us focus now on the evaluation of the volume and moment of inertia for a two-dimensional thin-walled wing section with constant thickness t. In particular, let us consider a discretization of the airfoil perimeter within N points indicated by $\mathbf{P}_i$. For a sufficiently close spacing, the airfoil segment bounded between $\mathbf{P}_i$ and $\mathbf{P}_{i+1}$ can be approximated as a rectangle with dimensions $|\mathbf{P}_i - \mathbf{P}_{i+1}|$ and t (see Fig. 1). Thus, as $t \ll c$, the total area is calculated as discrete sum of the infinitesimal rectangular contributions:

$$A(\mathbf{Y}) = t \sum_{i=1}^{N} |\mathbf{P}_i - \mathbf{P}_{i+1}|. \tag{6}$$

In a similar way, the polar moment of inertia J_{AC} can be calculated as the sum of the moment of inertia of each

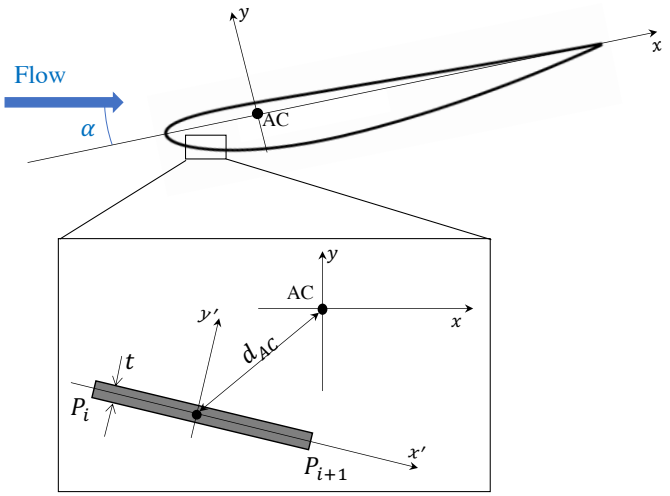

Fig. 1. Discretization of the thin-walled airfoil shape to calculate the volume and the moment of inertia.

segment with respect to the aerodynamic center (AC). Using the notation of Fig. 1, we have:

$$J_{AC}(\mathbf{Y}) = \sum_{i=1}^{N} J_{AC,\ i}(\mathbf{Y}). \tag{7}$$

With respect to a local reference frame $(x',\ y')$ oriented as in Fig. 1, the polar moment of inertia with respect to the axis z' passing through the centroid of the rectangle is:

$$J'_i = \frac{|\ \mathbf{P}_i - \mathbf{P}_{i+1}\ |\ t}{12}\left[t^2 + |\ \mathbf{P}_i - \mathbf{P}_{i+1}\ |^2\right]. \tag{8}$$

Finally, the polar moment of inertia with respect to the AC is related to the local moment of inertia by:

$$J_{AC,\ i}(\mathbf{Y}) = J'_i + d^2_{AC,i} t\ |\ \mathbf{P}_i - \mathbf{P}_{i+1}\ |\ . \tag{9}$$

B. XFOIL Flow solver

The evaluation of the velocity and pressure distribution around a 2D airfoil has been carried out using the XFOIL subroutine in MATLAB [16]. For a typical flow past the rear wing of an automobile, we can assume an incompressible and a subsonic flow field. For a given set of coordinates of a 2D shape, the XFOIL solver estimates the flow field using a viscous formulation of the Navier-Stokes equations. The boundary layers and wake are described with a two-lagged dissipation integral boundary layer formulation. It is assumed that at low angles of attack, the wake trajectory for a viscous calculation can be approximated as that from an inviscid solution. This significantly limits the accuracy of the ranges of angles of attack for a streamlined body. The advantage is the extremely low computation time for estimating the lift and drag coefficients for an airfoil. Although it is possible to implement a high-fidelity RANS solver, considering the computational limitations, the XFOIL solver was chosen due to its smooth integration with a MATLAB based optimization problem.

The input of the XFOIL subroutine are the 2D airfoil coordinates, the angle of attack α (in degrees), the chord Reynolds

number, the Mach number and other user-defined commands. The output includes the lift, drag and pitch-moment together with the pressure coefficients along the chord-line of the airfoil. For a flow past a 2D airfoil, the characteristic length is generally assumed to be the chord length of the airfoil, and hence the Reynolds number and the Mach number for a particular speed of an automobile can be estimated as follows:

$$Re = \frac{\rho U_\infty C}{\mu} \tag{10}$$

$$M_\infty = \frac{U_\infty}{a_\infty} \tag{11}$$

where, U_∞ is the freestream velocity and a_∞ is the speed of sound in air. For the current study, a freestream velocity of $U_\infty = 30$ m/s corresponding to an automobile speed of 108 kmph was selected. As a base case, the chord length of the airfoil was set to $c = 0.3$ m. Moreover, a low and a constant angle of attack of $\alpha = 3°$ was chosen in order to avoid the XFOIL-based inaccuracies resulting from the flow separation at the trailing edge. This sets up a simple subroutine to accurately estimate the lift and drag characteristics of a 2D airfoil.

IV. Results

A. Choice of the initial airfoil

In the reminder of this study, the NURBS parametrization will be used to change the shape of an airfoil through its control points in order to achieve the minimum of a given cost function in an iterative fashion. However, prior to the main optimization, an initial guessed airfoil for incompressible flow applications (and the related control polygon) must be chosen to start the iterations. To this aim, a target airfoil for incompressible flows (s1223rtl-il[1]) has been selected and the related control polygon has been determined from a dedicated preliminary optimization routine. Starting from a guessed distribution of control points, the upper and lower portions of the airfoil have been optimized on the s1223 upper and lower semi-profiles to obtain the control polygon; the subdivision of the optimization problem into two parts has been assessed in [1]. Said y_{ref} and y the vertical coordinates of the reference and the optimized airfoils respectively, the optimization problem has been formulated as in [1]:

$$\min_{Y} \; 2\epsilon_{\text{mean}} + \epsilon_{\text{max}}, \tag{12}$$

Where Y are the vertical coordinates of the control points. The functions ϵ_{mean} and ϵ_{max} represent the mean and maximum errors, defined as follows:

$$\epsilon_{\text{mean}} = \frac{1}{c}\int_0^c |y - y_{\text{ref}}| \mathrm{d}x; \tag{13}$$

$$\epsilon_{\text{max}} = \frac{1}{c}\max_x |y - y_{\text{ref}}| \tag{14}$$

and c is the chord length.

[1]The database with the airfoil coordinates is available at: http://airfoiltools.com.

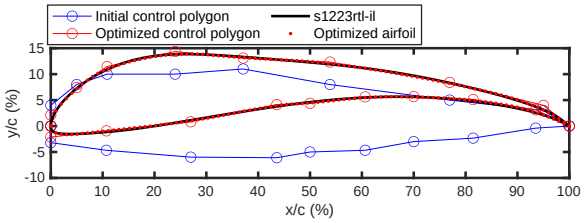

Fig. 2. Evaluation of the s1223rtl-il control polygon. The reference airfoil is depicted with black line, the optimized one with red dots and the related control polygon with empty red circles. The initial control polygon is reported with empty blue circles.

The y-coordinates of the control points have been iteratively changed through a gradient-based procedure in order to minimize the cost function. In contrast, the x-coordinates of the control points have been kept fixed (as in [1], [17]); also, for this optimization case, the weights have been set equal to 1 . The constraints of the present problem are:

$$\begin{aligned} Y_0 &= 0 \\ Y_n &= 0 \\ w_i &= 1 \end{aligned} \tag{15}$$

where the subscript 0 and n refer to the control points located either at the leading or trailing edge. The latter must be associated to zero values of Y and unitary values of the associated weights.

Equations (12, 13) and (14) have been numerically evaluated over 100 points equally spaced along the chord line. Both for the upper and the lower airfoil portions, 8 control points have been placed between leading and trailing edges; the NURBS order has been selected equal to: $p = 3$ to have continuity up to the second derivative. A gradient-based procedure based on the Sequential Quadratic Programming (SQP) approximation has been chosen to solve the non-linear constrained optimization problem ([18]). The resulting optimal control polygon is plotted in Fig. 2; here it appears that the reference s1223 airfoil is exactly matched by the optimized airfoil shape, with a final mean error value of: $\epsilon_{\text{mean}} = 5.96 \cdot 10^{-4}$ and a maximum error of: $\epsilon_{\text{max}} = 10^{-3}$.

B. Optimization results and discussion

As shown by equation 5, the total objective function is a linear combination of the airfoil cross-section area (proportional to the airfoil mass) and the inverse of the polar moment of inertia with respect to the aerodynamic center. The linear weights of these individual objective functions are varied to obtain the Pareto frontier of the total objective function. For the current problem, the values of the weights mentioned in the Table I were used, where each pair represents an optimization design point.

The optimization was performed on the initial S-1223 airfoil using the *fmincon* subroutine of MATLAB, with the earlier mentioned constraints to minimize volume and maximize polar moment of inertia. A subroutine named *get-airfoil* was developed to extract the airfoil coordinates from a set of NURBS control points using the procedure described in the

TABLE I
THE WEIGHTS OF THE OBJECTIVE FUNCTION

μ_1	$\mu_2 = (1 - \mu_1)$
0.1	0.9
0.14	0.86
0.24	0.76
0.3	0.7
0.5	0.5
0.7	0.3
0.9	0.1

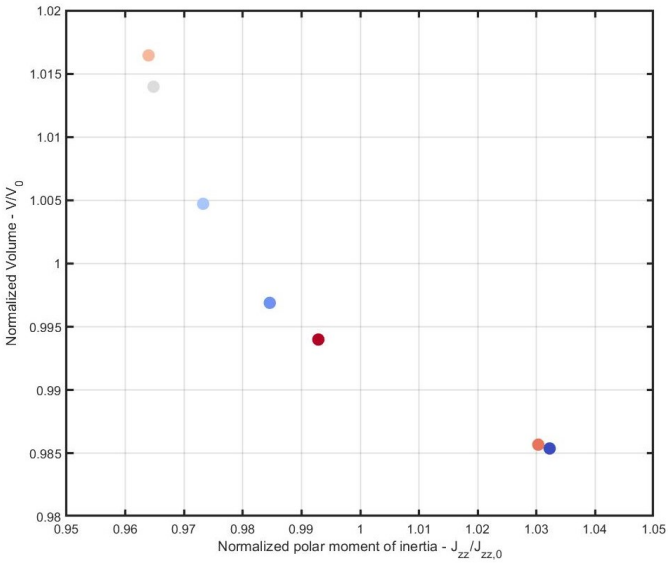

Fig. 3. The scatter plot of the normalized objective function values w.r.t. the initial airfoil, for all optimized shapes corresponding to each pair of weights in Table I.

section III. This subroutine is called to estimate the objective function values, aerodynamic characteristics and constraints from a set of NURBS control points. The normalized values of the objective functions of the final optimized airfoil for each of these pairs are plotted in Fig. 3. From this plot we can see how the optimization results are distributed along a well-defined Pareto frontier. The point $(1, 1)$ in the plot (not shown) corresponds to the initial airfoil (s1223). The color map of each point in the figure indicates the corresponding shape in the plot of all optimized airfoil shapes in 4. Although the percentage variation in the normalized values may not be significant, it is important to investigate the shape variation and the aerodynamic characteristics of each of the optimized airfoil shape.

The shapes of all corresponding optimized airfoils in Fig. 3 are shown in Fig. 4. The Pareto point with the minimal normalized volume V/V_0 is indeed the airfoil with the lowest thickness in the figure. Similarly, the airfoil with highest polar moment J_{AC} is the airfoil with the largest thickness. As mentioned in the problem formulation, the most important aerodynamic design parameters for a 2D airfoil are the lift and drag coefficients. The aerodynamic efficiency defined as the lift-to-drag ratio is also a crucial parameter while comparing airfoils with similar lift or drag coefficients. These parameters

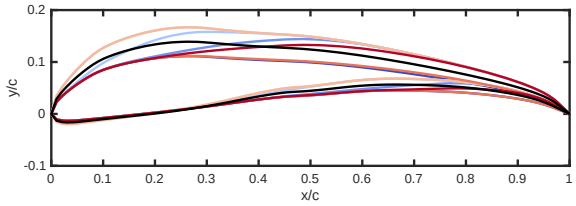

Fig. 4. The optimized airfoil shapes for each of the Pareto points. The colors indicate the corresponding points in the figure 3.

are reported here:

$$C_L = \frac{L}{\frac{1}{2}\rho U_\infty^2 A} \tag{16}$$

$$C_D = \frac{D}{\frac{1}{2}\rho U_\infty^2 A} \tag{17}$$

$$E = \frac{L}{D} = \frac{C_L}{C_D} \tag{18}$$

$$C_p(x/c) = \frac{p(x/c)}{\frac{1}{2}\rho U_\infty^2} \tag{19}$$

Here, c represents the airfoil chord length and A is the planar area of the wing, which is equal to the chord length for a 2D airfoil with a unit spanwise thickness. The values of the C_L, C_D and E against the inverse polar moment weight, μ_2 are plotted in Fig. 5. The results show that the maximum lift condition is achieved when the volume is largest, i.e. for the lowest weight value μ_1 of the volume. This is as expected since there is a greater curvature on the top half of the airfoil which increases the suction peak and eventually the lift. The airfoil section resulting in highest efficiency correspond to a weight of $\mu_2 = 0.24$, which has also the lowest drag coefficient. Overall, as the value of μ_2 increases, the airfoil thickness gets larger and the lift and drag coefficients increase, with a local maximum point for the aerodynamic efficiency, E corresponding to the local minimum of the drag coefficient at $\mu_2 = 0.3$.

To better clarify the relationship between the optimized airfoil shape and the aerodynamic characteristics, let us examine the coefficient of pressure distribution (C_p) over the airfoil section (Fig. 6). The C_p is plotted for the airfoils with maximum lift and with maximum aerodynamic efficiency. As expected, the thinner airfoil with maximum efficiency has a lower C_P distribution due to the compensation in the lift. As anticipated, the maximum lift airfoil shows a high pressure gradient whereas the one with maximum efficiency is much smoother towards the trailing edge.

V. CONCLUSIONS AND SUMMARY

In this work, the optimization of a rear-wing section for a high-performance car has been presented. The objective

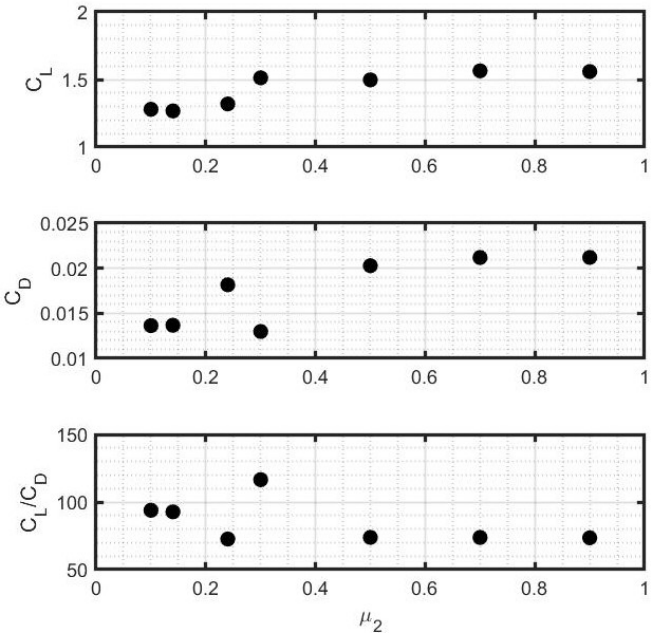

Fig. 5. The C_L, C_D and E values against the inverse polar moment weight, μ_2.

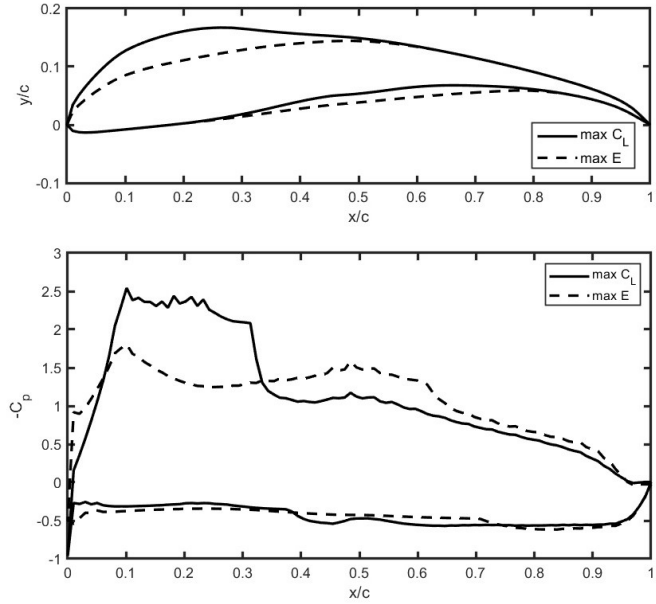

Fig. 6. Aifoil sections with maximum C_L and maximum E, along-with their respective $C_P(x/c)$ distribution. The maximum C_L corresponds to $\mu_2 = 0.9$ and the maximum E corresponds to $\mu_2 = 0.3$.

function expressed two opposite requirements, namely the minimization of the airfoil weight and the maximization of the moment of inertia in order to increase the torsional stiffness. The importance of these aspects has been highlighted in several literature studies (see e.g. [12], [15], [13]). Given the opposite nature of the two requirements, a multi-objective problem has been defined in order to find a set of non-dominated solutions distributed along a Pareto frontier. The constraints of the problem are given by the aerodynamic performance of the airfoil in terms of lift and drag coefficients. The airfoil shape has been iteratively modified during the optimization process by means of its NURBS parametrization ([7]); this is a very common strategy used in aerodynamic optimization ([3], [2], [1]) as it allows to control the local airfoil shape by means of a low number of control points (of the order of 10 for both the upper and the lower portions of the airfoil). The optimization has been ran through a gradient-based procedure in MATLAB with a very low computational cost. The initial design point was represented by a typical airfoil for automotive applications, whose control polygon has been obtained by a separated shape optimization process.

As a result, a Pareto frontier with 7 points has been obtained changing the relative weights associated to either one of the two objective functions; each optimized shape showed remarkable differences with respect to the initial airfoil. In particular, we focused our attention onto two optimized airfoils, i.e. the one with maximum lift coefficient and the one with maximum efficiency. It has been inferred that the maximum lift is obtained with the thicker airfoil due to the increase in the suction peak on the upper portion; this airfoil is associated to the largest moment of inertia obtained with a maximum value of the related weight in the optimization problem. On the other hand, the maximum efficiency is obtained for a relatively low-thickness airfoil when the mass reduction is associated with a large value of the optimization weight. In particular, the mass optimization leads to a reduction of the thickness which causes the decrease of the adverse pressure gradient on the rear part of the airfoil, thus the drag coefficient is reduced and the efficiency increases.

This project highlighted the importance of having a trade-off between different requirements during the optimization of an aerodynamic element. In particular, when the multi-optimization problem is posed from the structural standpoint, the aerodynamic performances follow as an outcome of the optimization procedure; this allows the designer to choose between different points along the Pareto frontier according to the desired aerodynamic features. Also, it is noteworthy that the present study represents an example of interaction between different computational tools (MATLAB and XFOIL), used in an iterative way to achieve the result. Although the computational cost has been kept low, the accuracy of the presented results was good enough to draw conclusions about the aerodynamic of the optimized airfoils.

VI. Acknowledgements

We acknowledge the MECH 6318 course instructor Dr. Jie Zhang and the teaching assistant Mr. Yuanzhi Liu for their continuous support during the project work.

References

[1] Y. Liang, X. Cheng, Z. Li, and J. Xiang, "Multi-objective robust airfoil optimization based on non-uniform rational b-spline (nurbs) representation," *Sci. China Technol. Sci.*, vol. 53, pp. 2708–2717, 2010.

[2] S. Painchaud-Ouellet, J.-Y. Trepanier, and D. Pelletier, "Airfoil shape optimization using nurbs representation under thickness constraint," *42nd AIAA Aerospace Sciences Meeting and Exhibit 5–8 January*, vol. 2095, 2004.

[3] J. Lepone, F. Guibault, J.-Y. Trepanier, and F. Pepin, "Optimized nonuniform rational b-spline geometrical representation for aerodynamic design of wings," *AIAA Journal*, vol. 39:11, pp. 2033–2041, 2001.

[4] S. Obayashi, "Multidisciplinary design optimization of aircraft wing planform based on evolutionary algorithms," in *SMC'98 Conference Proceedings. 1998 IEEE International Conference on Systems, Man, and Cybernetics (Cat. No. 98CH36218)*, vol. 4. IEEE, 1998, pp. 3148–3153.

[5] G. Venter and J. Sobieszczanski-Sobieski, "Multidisciplinary optimization of a transport aircraft wing using particle swarm optimization," *structural and Multidisciplinary optimization*, vol. 26, no. 1-2, pp. 121–131, 2004.

[6] Y. Zhang, X. Fang, H. Chen, S. Fu, Z. Duan, and Y. Zhang, "Supercritical natural laminar flow airfoil optimization for regional aircraft wing design," *Aerospace science and Technology*, vol. 43, pp. 152–164, 2015.

[7] L. Piegl and W. Tiller, *The NURBS book*. Springer Science & Business Media, 2012.

[8] K. R. Ram, S. Lal, and M. Rafiuddin Ahmed, "Low Reynolds number airfoil optimization for wind turbine applications using genetic algorithm," *Journal of Renewable and Sustainable Energy*, vol. 5, no. 5, 2013.

[9] J. D. Anderson Jr, *Fundamentals of aerodynamics*. Tata McGraw-Hill Education, 2010.

[10] D. Spink, "Nurbs matlab toolbox," 2018.

[11] "F1technical.net - formula one uncovered: https://www.f1technical.net/."

[12] J. Katz, "Aerodynamics of race cars," *Annu. Rev. Fluid Mech.*, vol. 38, pp. 27–63, 2006.

[13] A. Sunanda and M. S. Nayak, "Analysis of naca 2412 for automobile rear spoiler using composite material," *International Journal of Emerging Technology and Advanced Engineering*, vol. 3, no. 1, pp. 230–238, 2013.

[14] M. F. Samuels, "Structural weight comparison of a joined wing and a conventional wing," *Journal of Aircraft*, vol. 19, no. 6, pp. 485–491, 1982.

[15] D. W. Zingg and S. Elias, "Aerodynamic optimization under a range of operating conditions," *AIAA journal*, vol. 44, no. 11, pp. 2787–2792, 2006.

[16] L. Edelman, "Xfoil interface updated (https://www.mathworks.com/matlabcentral/fileexchange/49706-xfoil-interface-updated), matlab central file exchange. retrieved october 25, 2020." 2020.

[17] K. Takenaka, K. Nakahashi, S. Obayashi, and K. KisaMatsushima, "The application of mdo technologies to the design of a high performance small jet aircraft-lessons learned and some practical concerns," in *35th AIAA fluid dynamics conference and exhibit*, 2005, p. 4797.

[18] S. S. Rao, *Engineering Optimization: theory and practice*, 4th ed. Hoboken, New jersey: John Wiley & Sons, 2009, vol. 27, no. 1.